British Journal of Pharmacology (2008) 153, 1485–1494
 0007–1188/08 $30.00
www.brjpharmacol.org

RESEARCH PAPER

Identification of the α_{1L}-adrenoceptor in rat cerebral cortex and possible relationship between α_{1L}- and α_{1A}-adrenoceptors

S Morishima, F Suzuki, H Yoshiki, AS Md Anisuzzaman, ZS Sathi, T Tanaka and I Muramatsu

Division of Pharmacology, Department of Biochemistry and Bioinformative Sciences, School of Medicine, University of Fukui, Eiheiji, Fukui, Japan

Background and purpose: In addition to α_{1A}, α_{1B} and α_{1D}-adrenoceptors (ARs), putative α_{1L}-ARs with a low affinity for prazosin have been proposed. The purpose of the present study was to identify the α_{1A}-AR and clarify its pharmacological profile using a radioligand binding assay.
Experimental approach: Binding experiments with [^{3}H]-silodosin and [^{3}H]-prazosin were performed in intact tissue segments and crude membrane preparations of rat cerebral cortex. Intact tissue binding assays were also conducted in rat tail artery.
Key results: [^{3}H]-silodosin at subnanomolar concentrations specifically bound to intact tissue segments and membrane preparations of rat cerebral cortex at the same density (approximately 150 fmol mg^{-1} total tissue protein). The binding sites in intact segments consisted of α_{1A} and α_{1L}-ARs that had different affinities for prazosin, while the binding sites in membranes showed an α_{1A}-AR-like profile having single high affinity for prazosin. [^{3}H]-prazosin also bound at subnanomolar concentrations to α_{1A} and α_{1B}-ARs but not α_{1L}-ARs in cerebral cortex; the binding densities being approximately 200 and 290 fmol mg^{-1} protein in the segments and the membranes, respectively. In the segments of tail artery, [^{3}H]-silodosin only recognized α_{1A}-ARs, whereas [^{3}H]-prazosin bound to α_{1A} and α_{1B}-ARs.
Conclusions and implications: The present study clearly reveals the presence of α_{1L}-ARs as a pharmacologically distinct entity from α_{1A} and α_{1B}-ARs in intact tissue segments of rat cerebral cortex but not tail artery. However, the α_{1L}-ARs disappeared after tissue homogenization, suggesting their decomposition and/or their pharmacological profile changes to that of α_{1A}-ARs.
British Journal of Pharmacology (2008) **153,** 1485–1494; doi:10.1038/sj.bjp.0707679; published online 28 January 2008

Keywords: α_{1L}-adrenoceptor; α_{1A} and α_{1B}-adrenoceptors; rat cerebral cortex; rat tail artery; tissue segment binding assay with [^{3}H]-silodosin and [^{3}H]-prazosin

Abbreviations: AR, adrenoceptor; BMY 7378, (8-[2-[4-(2-methoxyphenyl)-1-piperazinyl]ethyl]-8-azaspiro[4,5]decane-7,9-dione dihydrochloride; RS-17053, *N*-[2-(2-cyclopropylmethoxyphenoxy)ethyl]-5-chloro-α,α-dimethyl-1*H*-indole-3-ethamine hydrochloride

Introduction

α_1-Adrenoceptors (ARs) are widely distributed in the brain and peripheral organs and play a number of important roles in many physiological processes (Hieble, 2000; Michelotti *et al*., 2000). At present, three distinct subtypes of α_1-ARs (α_{1A}, α_{1B} and α_{1D}) have been cloned and identified pharmacologically in native tissues (Hieble *et al*., 1995; Michel *et al*., 1995; Zhong and Minneman, 1999). These three subtypes show different pharmacological profiles for various drugs, although the classical α_1-AR antagonist prazosin shows a high (subnanomolar) affinity for all three subtypes. The α_{1A}-AR shows higher affinities for silodosin (previously known as KMD-3213, (−)-1-(3-hydroxypropyl)-5-[(2*R*)-2-({2-[2-(2,2,2-trifluoroethoxy)phenoxy]ethyl}amino)propyl]-2,3-dihydro-1*H*-indole-7-carboxamide), RS-17053 (*N*-[2-(2-cyclopropylmethoxyphenoxy)ethyl]-5-chloro-α,α-dimethyl-1*H*-indole-3-ethamine hydrochloride) and 5-methylurapidil than the α_{1B} and α_{1D}-ARs (Ford *et al*., 1996; Kenny *et al*., 1997; Honner and Docherty, 1999; Murata *et al*., 1999). Tamsulosin has a high affinity for all three AR subtypes, although a slightly low affinity for the α_{1B}-AR (Testa *et al*., 1997; Muramatsu *et al*., 1998b). BMY 7378 (BMY 7378, (8-[2-[4-(2-methoxyphenyl)-1-piperazinyl]ethyl]-8-azaspiro[4,5]decane-7,9-dione dihydrochloride) is an α_{1D}-selective antagonist (Goetz *et al*., 1995). In addition to these three α_1-ARs, the presence of another subtype (the putative α_{1L}-AR) has been proposed (Muramatsu *et al*., 1990).

Correspondence: Professor I Muramatsu, Division of Pharmacology, Department of Biochemistry and Bioinformative Sciences, School of Medicine, University of Fukui, Eiheiji, Fukui 910-1193, Japan.
E-mail: muramatu@u-fukui.ac.jp
Received 21 November 2007; accepted 12 December 2007; published online 28 January 2008

The α_{1L}-AR shows a unique pharmacological profile: low affinity for prazosin, RS-17053 and 5-methylurapidil but high affinity for silodosin and tamsulosin (Muramatsu *et al*., 1995, 1998a; Ford *et al*., 1996; Murata *et al*., 1999). The α_{1L}-AR has been detected in various tissues, such as the rabbit thoracic aorta (Oshita *et al*., 1993), rat and human vas deferens (Ohmura *et al*., 1992; Amobi *et al*., 2002), rabbit iris (Nakamura *et al*., 1999; Suzuki *et al*., 2002) and rabbit, rat, guinea-pig and human prostate (Muramatsu *et al*., 1994; Hiraoka *et al*., 1995, 1999; Ford *et al*., 1996; Van der Graaf *et al*., 1997; Morishima *et al*., 2007), rat small mesenteric arteries (Stam *et al*., 1999) and canine subcutaneous arteries (Argyle and McGrath, 2000). α_{1L}-ARs have been identified primarily by functional studies. However, the corresponding gene has not yet been cloned, even though many trials of candidate genes have been carried out, including splicing variants of α_1-*AR* genes and heterodimeric expression of different subtypes. Hence, Ford *et al*. (1997) have suggested that the α_{1L}-AR may be a functional phenotype of the α_{1A}-AR. More recently, results from research into receptor phenotypes have suggested that several G-protein-coupled receptors may be able to express another phenotype under different environmental conditions (Muramatsu *et al*., 2005; Nelson and Challiss, 2007). Thus, a more detailed characterization of the α_{1L}-AR is required, particularly under conditions close to a natural environment.

Most binding studies have been successfully performed using tissue-derived microsomal or crude membrane preparations (Bylund and Toews, 1993). Recently, we developed a tissue segment binding method for determining ligand binding and demonstrated that, in contrast to conventional membrane binding methods, the tissue segment binding method avoids the change in the receptor environment induced by homogenization (Muramatsu *et al*., 2005). Using this tissue segment binding method and [^{3}H]-silodosin (a new radioligand selective for α_{1A}- and α_{1L}-ARs), Hiraizumi-Hiraoka *et al*. (2004) and Morishima *et al*. (2007) have clearly demonstrated that the α_{1L}-AR is a distinct binding site different from α_{1A}-ARs in the rabbit ear artery and human prostate.

The aims of the present study were to compare the binding sites of two radioligands ([^{3}H]-prazosin and [^{3}H]-silodosin) and to explore the α_{1L}-AR as a distinct binding entity different from the already known α_1-ARs. Experiments were performed in the rat cerebral cortex and tail artery where the presence of α_{1A}- and α_{1B}-ARs has been demonstrated in conventional membrane binding and functional studies, and at the mRNA level (Morrow and Creese, 1986; Hanft and Gross, 1989; Lachnit *et al*., 1997; Yang *et al*., 1997; Michelotti *et al*., 2000; Taki *et al*., 2004; Tanaka *et al*., 2004). In order to detect α_{1A}- and α_{1L}-ARs without contamination with α_{1B}- and α_{1D}-ARs, [^{3}H]-silodosin was used and the binding profile was compared with that of a classical radioligand selective for α_{1A}-, α_{1B}- and α_{1D}-ARs, [^{3}H]-prazosin. The binding results obtained in the present study clearly showed the coexistence of α_{1A}-, α_{1B}- and α_{1L}-ARs in the intact tissue segments of rat cerebral cortex and of α_{1A} and α_{1B} in the rat tail artery segments. The α_{1L}-AR was only detected in tissue segments by [^{3}H]-silodosin, but it changed to an α_{1A}-like profile upon/after homogenization.

Methods

Animals and tissue isolation

Male Wistar rats (Charles River Japan Inc., Yokohama, Japan) weighing approximately 300 g were used. Animals were housed under a 12-h light/dark cycle (lights on 0800 hours; lights off 2000 hours) and had free access to standard laboratory food and tap water. The room temperature and relative humidity were strictly regulated at 21–25 °C and 40–70%, respectively. The present study was performed according to the Guidelines for Animal Experiments, University of Fukui.

Rats were anaesthetized by an intraperitoneal injection of sodium pentobarbital (50 mg kg^{-1}) and killed by cervical dislocation. The brain cortex and tail artery were rapidly excised and placed in a modified Krebs–Henseleit solution (composition mM: NaCl, 120.7; KCl, 5.9; $MgCl_2$, 1.2; $CaCl_2$, 2.0; NaH_2PO_4, 1.2; $NaHCO_3$, 25.5 and D-glucose, 11.5). The modified Krebs–Henseleit solution was gassed with a mixture of 95% O_2 and 5% CO_2 and maintained at 4 °C (pH = 7.4).

Tissue segment binding experiments with [^{3}H]-silodosin and [^{3}H]-prazosin

Tissue segment binding was performed as described previously (Muramatsu *et al*., 2005). Briefly, under the dissecting microscope, the isolated cerebral cortex and tail artery of rat were cut into small pieces (approximately 2.5 × 2.5 × 3 mm for cortex and 3.5 mm in length for tail artery). Each piece was incubated with [^{3}H]-silodosin or [^{3}H]-prazosin for 15–16 h at 4 °C in 1 ml of a Krebs incubation buffer. The duration of the incubation had been determined in preliminary studies such that the time course of the specific binding reached a plateau. The composition of the Krebs incubation buffer was essentially the same as a modified Krebs–Henseleit solution except that the $NaHCO_3$ concentration was reduced to 10.5 mM to adjust pH to 7.4 in air. The osmolarity of the Krebs incubation buffer was adjusted by adding NaCl. In binding saturation experiments, concentrations of [^{3}H]-silodosin (50–1000 or 2000 pM) and [^{3}H]-prazosin (50–1000 pM) were used. Binding-competition experiments were performed at 500 pM [^{3}H]-silodosin and 300 pM [^{3}H]-prazosin in the cortex and 200 pM [^{3}H]-silodosin and 500 pM [^{3}H]-prazosin in the tail artery, respectively. After incubation, the tissue segments were quickly moved into a plastic tube containing 1.5 ml of incubation buffer and vortexed at 4 °C for 1 min. By this procedure, most of the unbound radioligand was released from the segments into the washing buffer and absorbed to plastic tube (Muramatsu *et al*., 2005). The pieces were then blotted and dissolved in 0.3 M NaOH solution to estimate the radioactivity and protein content. The specific binding was determined by subtracting the amount bound in the presence of 30 μM phentolamine from the total radioactivity bound per mg protein. Initially, the same amount of specific binding sites was observed using high concentrations of various α_1-AR agonists and antagonists (Figure 1). Thus, the binding sites measured in the present studies appeared to reflect the specific bindings of the radioligands to α_1-ARs and not simply the nonspecific accumulation of the radioligands in the tissue. As nonspecific

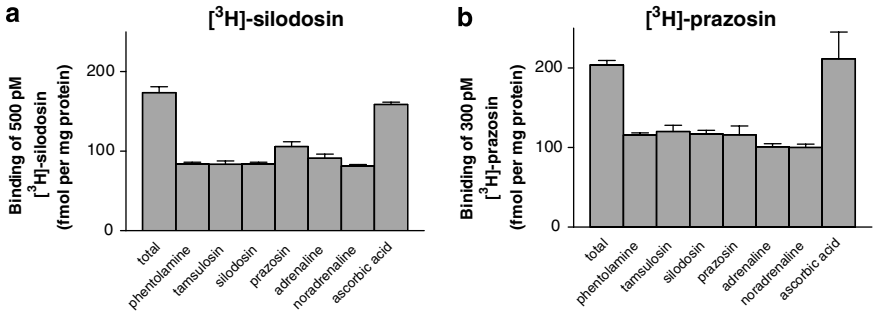

Figure 1 Effects of various drugs on the binding of 500 pM [^{3}H]-silodosin (**a**) and 300 pM [^{3}H]-prazosin (**b**) in intact segments of rat cerebral cortex. The concentrations of drugs used are as follows: 30 μM phentolamine, 1 μM tamsulosin, 1 μM silodosin, 1 μM prazosin, 100 μM adrenaline, 100 μM noradrenaline and 0.01% ascorbic acid. Adrenaline and noradrenaline were incubated in the presence of 0.01% ascorbic acid. 'Total' indicates the binding in the absence of any drugs. Binding capacity, fmol per mg total tissue protein, was calculated from the specific activity of each radioligand. The results shown are the mean ± s.e.mean of 4–5 determinations.

binding in the presence of adrenaline, known to be hydrophilic, was equivalent to that in the presence of the other ligands, the specific binding sites of the radioligands used in these experiments were likely to be neither accumulation into the cells nor intracellular binding sites (MacKenzie *et al*., 2000). Experiments were performed in duplicate at each concentration of radioligand for a saturation experiment or at each concentration of competing ligand for a binding-competition experiment. Radioactivity was measured by liquid scintillation counting using a water-miscible scintillation fluid (ULTIMA GOLD, Packard Bioscience, Groningen, The Netherlands). The amount of protein in each tissue segment was measured using a Bio-Rad Protein Assay kit (Bio-Rad Japan, Tokyo, Japan).

Membrane binding experiments with [^{3}H]-silodosin and [^{3}H]-prazosin

The isolated cerebral cortex was minced with scissors and homogenized in 40 volumes (v/w) of Krebs incubation buffer using a polytron homogenizer (specify setting 8, 5 × 20 s at 4 °C). The Krebs incubation buffer was the same as that used in the tissue segment binding experiments but proteinase inhibitors (Complete, EDTA-free tablet, Roche, Penzberg, Germany) were added upon homogenization. The tissue homogenate was subjected to centrifugation at 1000 *g* for 10 min at 4 °C. The supernatant was filtered through four layers of gauze (Type I) and then centrifuged at 80 000 *g* for 30 min at 4 °C. The resulting pellet was resuspended in the Krebs incubation buffer without proteinase inhibitors and used as crude membrane preparations for binding experiments.

In binding experiments, the crude membranes were incubated for 4 h at 4 °C in 1 ml of Krebs incubation buffer. In binding saturation experiments, [^{3}H]-silodosin (50–1000 pM) and [^{3}H]-prazosin (50–1000 or 5000 pM) were used. In binding-competition experiments, the membranes were incubated with 500 pM [^{3}H]-silodosin and 3000 pM [^{3}H]-prazosin in the absence or presence of unlabelled competing ligands. Reactions were terminated by rapid filtration using a Brandel cell harvester onto Whatman GF/C filters presoaked in 0.3% polyethyleneimine for 15 min, and the filters were then washed three times with 5 ml of Krebs incubation buffer. The resulting filters were dried and the trapped radioactivity was quantified by liquid scintillation counting. Nonspecific binding of [^{3}H]-silodosin and [^{3}H]-prazosin was defined as the binding in the presence of 30 μM phentolamine. Experiments were performed in duplicate at each concentration of radioligand for a binding saturation experiment or at each concentration of competing ligand for a binding-competition experiment. The protein contents of homogenates before centrifugation and of the crude membrane fractions were measured using a Bio-Rad Protein Assay kit (Bio-Rad Japan, Tokyo, Japan).

Data analysis

Binding data were mainly analysed by Graph Pad PRISM (Ver. 3, Graph Pad Software, San Diego, CA, USA). For Hill plot and pseudo-Hill plot analyses, Origin (Ver 7.5, OriginLab Co., Northampton, MA, USA) was used. In saturation binding studies, data were fitted by a one-site saturation binding isotherm. To validate the one-site model, Hill coefficients were calculated from Hill plots.

In competition studies, the data were first fitted to a one- and then a two-site model, and if the residual square sums were significantly less for a two-site fit of the data than for a one-site ($P<0.05$ as determined by F-test), then a two-site model was accepted. Slopes of pseudo-Hill plots were also determined for some competitors to validate one- or two-site fitting.

The number of α_1-ARs in the rat cerebral cortex and tail artery was presented as maximum binding capacity per mg of total tissue protein (fmol per mg of total tissue protein). That is, in the case of conventional binding experiments with membrane fractions of cerebral cortex, the proteins in the homogenates before fractionation were measured as total tissue protein. Usually, the protein yield of the membrane fractions was 1 mg from 1.9 to 2.1 mg of total tissue protein of rat cerebral cortex. For intact tissue binding, the tissues were dissolved in 0.3 M NaOH solution and the total protein content was measured as mentioned above.

Data are represented as the mean ± s.e.mean of *n* number of experiments. Binding data in Figure 1 were compared by one-way ANOVA followed by Scheffe's *post hoc* test. Values for maximum binding capacity were compared between tissue segments and membranes by Student's *t*-test. A

probability of less than 0.05 was considered significant. Confidence intervals (95%) were also given for the Hill and pseudo-Hill coefficients.

Drugs

The drugs used and their sources were: silodosin and tamsulosin from Kissei Pharmaceutical Co. Ltd (Matsumoto, Japan); phentolamine hydrochloride, prazosin hydrochloride from Sigma (St Louis, MO, USA); *l*-adrenaline bitartrate, *l*-noradrenaline bitartrate (Nacalai Tesque, Kyoto, Japan); 5-methylurapidil, BMY 7378 and RS-17053 from Research Biochemicals International (Natic, MA, USA). Prazosin was dissolved in 50% ethanol and diluted with binding buffer in binding experiments. The stock solution of silodosin and RS-17053 were prepared with dimethylsulphoxide and then diluted with binding buffer. [^{3}H]-silodosin (specific activity 1.92 TBq mmol^{-1}) was manufactured by GE Healthcare UK (Buckinghamshire, UK), analysed on 10 October 2006, and provided by Kissei Pharmaceutical Co. Ltd. The radioligand was stored at −30 °C in methanol solution, under which conditions it is considered to be stable for more than a year.

Results

Rat cerebral cortex

To confirm that the specific binding of [^{3}H]-silodosin determined by the tissue segment binding method reflects the density of α_1-ARs in rat cortex and that it is not significantly affected by the nonspecific accumulation of the radioligand into the tissue, we first incubated the intact segments of rat cerebral cortex with 500 pM [^{3}H]-silodosin in the absence and presence of high concentrations of various α-AR ligands (phentolamine, tamsulosin, silodosin, prazosin, adrenaline and noradrenaline). Similar experiments were also performed using 300 pM [^{3}H]-prazosin, and the results were compared. Figure 1a shows the binding of [^{3}H]-silodosin obtained after 15–16 h incubation at 4 °C. Nonspecific bindings determined by co-incubating the tissues with high concentrations of α_1-AR ligands were similar and were approximately 50% of the total [^{3}H]-silodosin binding. This meant that all the α-AR ligands used competed equally with [^{3}H]-silodosin at its binding sites, and thus the number of sites estimated from the value of [^{3}H]-silodosin binding, in the absence of any other ligands minus the number obtained after co-incubation with various ligands, could be reasonably determined as specific binding to the α_1-ARs. Similar experiments were conducted using [^{3}H]-prazosin (Figure 1b). Nonspecific binding obtained in the experiments did not vary much between the drugs co-incubated, similar to the experiments with [^{3}H]-silodosin, although the proportion of nonspecific binding was slightly higher. It is notable that similar binding was obtained even when adrenaline, known to be hydrophilic and membrane-impermeable, was used, suggesting that the binding of both radioligands may reflect receptors on the surface plasma membrane. In the following experiments, nonspecific binding was determined as the binding in the presence of 30 μM phentolamine.

In the saturation binding experiments, [^{3}H]-silodosin (50–1000 pM) bound to tissue segments and membrane preparations of rat cerebral cortex in a concentration-dependent manner (Figures 2a and b). The Hill coefficients were

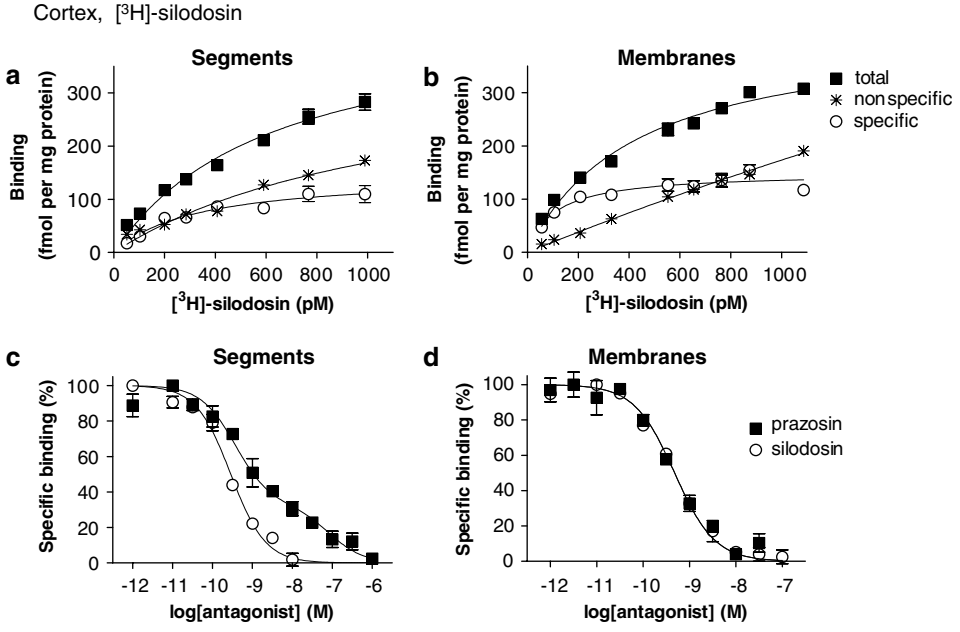

Figure 2 [^{3}H]-silodosin binding to rat cerebral cortex. (**a** and **b**) Saturation curves for [^{3}H]-silodosin binding in intact tissue segments and crude membranes of rat cerebral cortex, respectively. Ordinate scale represents binding per mg total tissue protein. The specific binding was determined by subtracting the amount bound in the presence of 30 μM phentolamine (nonspecific binding) from the total amount bound. (**c** and **d**) Competition curves for effects of prazosin and silodosin on [^{3}H]-silodosin (500 pM) binding sites in the intact segments and crude membranes, respectively. Each point represents the mean of duplicate determinations. Each figure is representative of similar results obtained in four other experiments.

0.89 ± 0.07 (95% confidence interval: 0.75–1.03) and 0.84 ± 0.08 (0.68–1.01) for tissue segments and membrane preparations, respectively, and it was supposed that [^{3}H]-silodosin bound to a single class of sites, as their 95% confidence interval include unity. The dissociation constant and maximal binding capacity (B_{max}) were 354 ± 31 pM and 155 ± 7 fmol mg^{-1} total tissue protein in the segments ($n = 5$) and 181 ± 46 pM and 154 ± 8 fmol mg^{-1} total tissue protein in the membrane preparations ($n = 5$), respectively. Thus, there was no significant difference in the number of [^{3}H]-silodosin binding sites between tissue segments and membrane preparations (Figure 3a).

The pharmacological profiles of [^{3}H]-silodosin binding sites in the tissue segments and the membrane preparations were examined in competition binding studies using several drugs. Competition curves for prazosin, RS-17053 and 5-methylurapidil in the tissue segments were clearly biphasic better fitted to a two-site model in computer analysis (Figure 2c for prazosin), and the proportion of high-affinity sites was 60 ± 6% (Figure 3a, Table 1). The slope factor in the pseudo-Hill plot analysis was −0.41 ± 0.02 (−0.37 to −0.45) for prazosin, which also indicates the existence of two affinity sites for prazosin. However, in the membrane preparations, prazosin, RS-17053 and 5-methylurapidil showed monophasic competition curves with high affinity (Figure 2d for prazosin, Table 1). The slope factor in the pseudo-Hill plot analysis was −0.94 ± 0.08 (−0.78 to −1.10) for prazosin, indicating a single affinity site for prazosin in the membrane preparations. In contrast to prazosin, silodosin, tamsulosin and BMY 7378 competed monophasically for the [^{3}H]-silodosin binding in both tissue segments and membrane preparations (Figures 2c and d for silodosin, Table 1). The slope factors for silodosin in the pseudo-Hill plot analyses were −0.83 ± 0.08 (−0.69 to −0.99) and −0.82 ± 0.09 (−0.64 to −1.01) in tissue segments and membrane binding, respectively, indicating a single affinity site for silodosin in both preparations.

[^{3}H]-prazosin also bound to the segments and crude membrane preparations of rat cerebral cortex in a concentration-dependent manner (Figures 4a and b). The proportion of nonspecific binding was significantly higher in tissue segments than in the membrane preparations; thus, low concentrations of [^{3}H]-prazosin (50–1000 pM) were used in the tissue segment binding assay. The saturation isotherm suggested a single class of [^{3}H]-prazosin binding sites in the segments ($K_d = 281 \pm 17$ pM, $B_{max} = 198 \pm 8$ fmol mg^{-1} total tissue protein, $n = 5$). The Hill coefficient was 1.01 ± 0.12 (0.77–1.24). In the membranes, the specific binding of [^{3}H]-prazosin showed a tendency to increase slightly up to 5000 pM of [^{3}H]-prazosin, but computer analysis of the saturation curve fitted to a single class of binding sites ($K_d = 123 \pm 22$ pM, $B_{max} = 290 \pm 9$ fmol mg^{-1} total tissue protein) and the Hill coefficient was close to unity (0.97 ± 0.14, 95% confidence interval: 0.70–1.23). Thus, a significantly higher number of [^{3}H]-prazosin binding sites was estimated in the membranes as compared with the segments ($P < 0.01$, Figure 3a right). The [^{3}H]-prazosin binding sites in the segments and the membranes were biphasically competed for by silodosin, RS-17053 and 5-methylurapidil, whereas prazosin and BMY 7378 showed the monophasic competition curves with high or low affinity, respectively (Figure 4d for silodosin and prazosin, Table 1). The slope factors in the pseudo-Hill plot analyses of tissue segment binding for silodosin and prazosin were −0.48 ± 0.02 (−0.44 to −0.51)

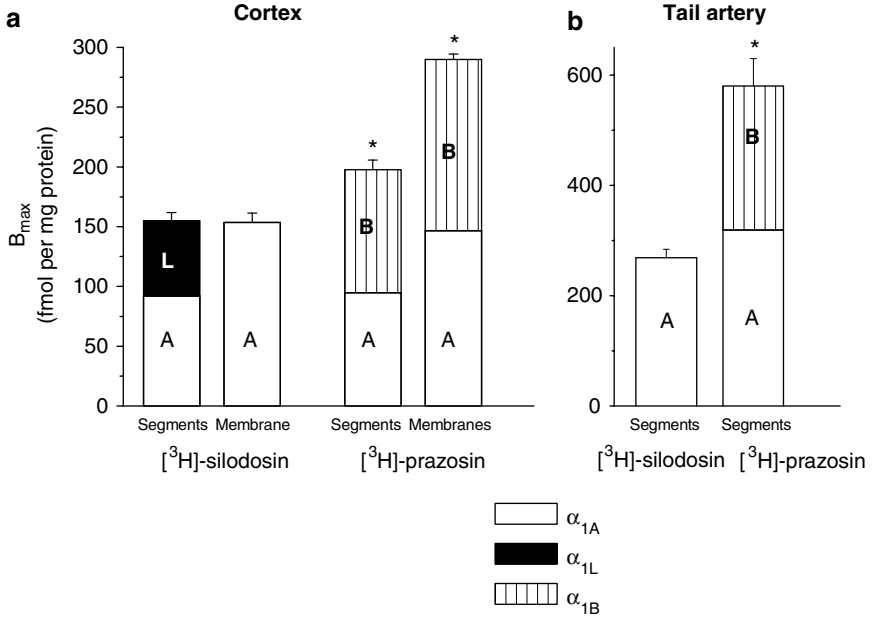

Figure 3 The binding capacity and pharmacological profile of [^{3}H]-silodosin and [^{3}H]-prazosin binding sites in rat cerebral cortex (**a**) and tail artery (**b**). High- and low-affinity sites for prazosin at [^{3}H]-silodosin binding sites were represented as α_{1A} (A) and α_{1L} (L), respectively. Likewise, the number of α_{1A} (A) and α_{1B} (B) ARs was estimated from the proportions of high- and low-affinity sites for silodosin at [^{3}H]-prazosin binding sites, respectively (see the text for further details). B_{max} values represent the mean ± s.e.mean of 4–5 experiments. Segments: intact tissue segment binding. Membranes: crude membrane binding. *Significantly different from [^{3}H]-silodosin binding sites ($P < 0.05$). B_{max}, maximal binding capacity.

Table 1 Binding affinities for α_1-AR antagonists at [^{3}H]-silodosin and [^{3}H]-prazosin binding sites in rat cerebral cortex

Drug	*[^{3}H]-silodosin Segments* $pK_{i\,high}$ *(%high)*	$pK_{i\,low}$	*Membranes* pK_i	*[^{3}H]-prazosin Segments* $pK_{i\,high}$ *(%high)*	$pK_{i\,low}$	*Membranes* $pK_{i\,high}$ *(%high)*	$pK_{i\,low}$
Prazosin	9.9 ± 0.2 (60 ± 6%)	7.8 ± 0.3	10.0 ± 0.2	9.9 ± 0.2		10.2 ± 0.1	
Silodosin	9.8 ± 0.3		9.9 ± 0.1	9.9 ± 0.3 (48 ± 3%)	7.9 ± 0.3	10.0 ± 0.2 (51 ± 3%)	8.1 ± 0.2
Tamsulosin	9.8 ± 0.2		10.0 ± 0.1	9.9 ± 0.1		10.3 ± 0.1	
BMY 7378	6.3 ± 0.2		6.5 ± 0.1	6.2 ± 0.2		6.3 ± 0.2	
RS-17053	8.7 ± 0.2 (57 ± 3%)	6.8 ± 0.2	9.1 ± 0.2	8.9 ± 0.3 (45 ± 4%)	7.8 ± 0.2	9.0 ± 0.2 (54 ± 4%)	7.1 ± 0.2
5-Methylurapidil	9.2 ± 0.3 (55 ± 4%)	8.2 ± 0.3	9.1 ± 0.3	8.9 ± 0.3 (45 ± 4%)	7.4 ± 0.2	9.4 ± 0.4 (52 ± 5%)	7.8 ± 0.3

Abbreviations: %high, proportion of high affinity sites; ND, not determined; $pK_{i\,high}$ and pK_{low}, negative logarithm of the equilibrium constants (pK_i) at high and low affinity sites for tested drugs.
Competitive binding experiments with intact tissue segments and crude membrane preparations were carried out at 500 pM [^{3}H]-silodosin or 300 pM [^{3}H]-prazosin. Data represent mean ± s.e.mean of 4–5 experiments.

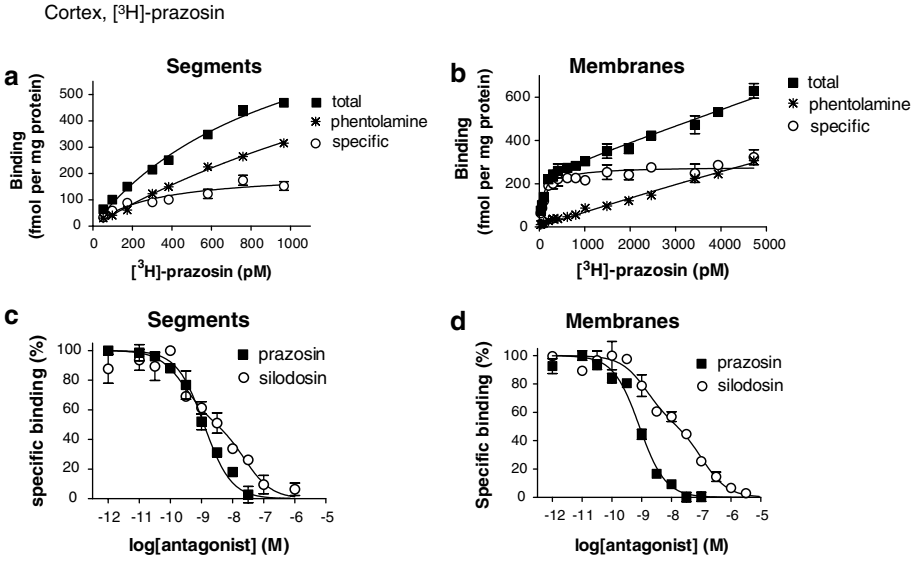

Figure 4 Saturation curve for [^{3}H]-prazosin in the intact tissue segments (**a**) and crude membrane preparations (**b**) of rat cerebral cortex, and competition curves for prazosin and silodosin at 300 and 3000 pM [^{3}H]-prazosin binding sites in the intact tissue segments (**c**) and membranes (**d**), respectively. Each figure is representative of similar results obtained in four other experiments.

and −0.91 ± 0.05 (−0.81 to −1.01), respectively, and those of the membrane binding were −0.62 ± 0.07 (−0.58 to −0.75) and −0.90 ± 0.09 (−0.73 to −1.07), supporting the evidence that two affinity sites exist for silodosin, but one for prazosin.

Rat tail artery

[^{3}H]-silodosin and [^{3}H]-prazosin bound to the segments of rat tail artery in a concentration-dependent manner (Figures 5a and b). Analysis of the saturation curves revealed the binding to be 269 ± 15 fmol mg^{-1} protein and the affinity of 173 ± 24 pM ($n = 4$) for [^{3}H]-silodosin, whereas a greater density of [^{3}H]-prazosin binding sites was estimated ($B_{max} = 580 \pm 50$ fmol mg^{-1} total tissue protein, $K_d = 381 \pm 11$ pM, $n = 4$) (Figure 3b). In competition experiments, the binding sites of [^{3}H]-silodosin were simply competed for by prazosin, silodosin, tamsulosin, RS-17053 and 5-methylurapidil with their high affinities and by BMY 7378 with a low affinity (Figure 5c for silodosin and prazosin, Table 2). On the other hand, [^{3}H]-prazosin binding sites were biphasically competed for by silodosin, RS-17053 and 5-methylurapidil (Figure 5d for silodosin and prazosin; Table 2). Analyses by Hill plots and pseudo-Hill plots supported these fitting data, as described in the legend of Figure 5.

Discussion

Prazosin has a high affinity for α_{1A}-, α_{1B}- and α_{1D}-ARs (Hancock, 1996; Murata *et al*., 1999; Hiraizumi-Hiraoka *et al*., 2004), whereas silodosin shows high selectivity to α_{1A}- and α_{1L}-ARs (Murata *et al*., 1999, 2000; Hiraizumi-Hiraoka *et al*., 2004). As these drugs show such different subtype selectivity, the binding sites of both [^{3}H]-prazosin and [^{3}H]-silodosin were compared in the cerebral cortex and tail artery of rats. In the rat cerebral cortex, the presence of

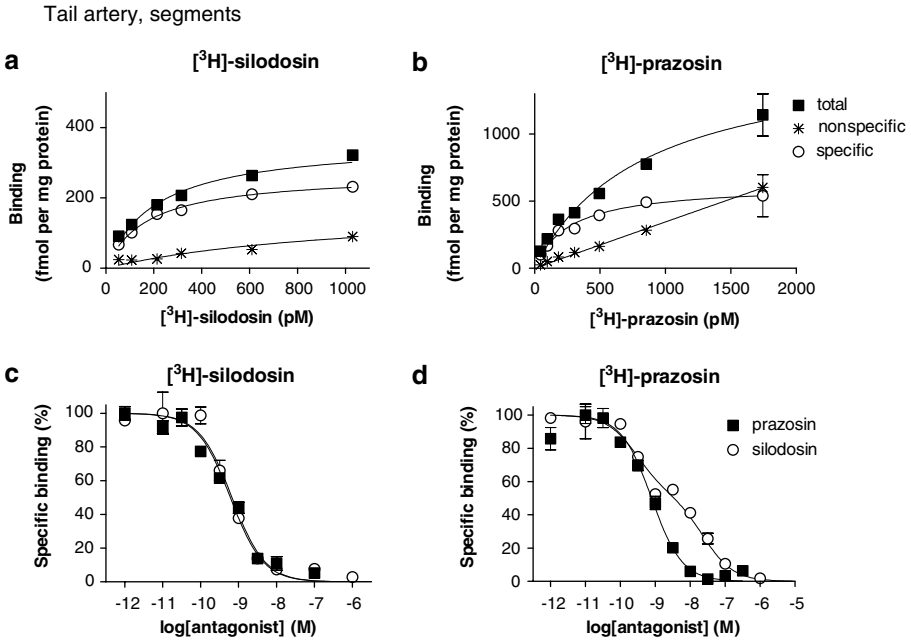

Figure 5 Saturation curves for [^{3}H]-silodosin (**a**) and [^{3}H]-prazosin (**b**), and competition curves for prazosin and silodosin at 200 pM [^{3}H]-silodosin (**c**) and 500 pM [^{3}H]-prazosin (**d**) binding sites in the intact segments of rat tail artery. Each figure is representative of similar results obtained in 3–4 other experiments. Hill coefficients of the saturation binding curves of [^{3}H]-silodosin and [^{3}H]-prazosin were 0.99 ± 0.04 (0.92–1.07) and 0.99 ± 0.05 (0.90–1.08), respectively. Slope factors (95% confidence interval) in the pseudo-Hill plot of the competition curves for silodosin and prazosin were −0.95 ± 0.08 (−0.79 to −1.10) and −0.86 ± 0.13 (−0.69 to −1.11) at [^{3}H]-silodosin binding sites, and −0.66 ± 0.05 (−0.56 to −0.76) and −1.11 ± 0.06 (−0.99 to −1.23) at [^{3}H]-prazosin binding sites, respectively.

Table 2 Binding affinities for α_1-AR antagonists at [^{3}H]-silodosin and [^{3}H]-prazosin binding sites in rat tail artery

Drug	*[^{3}H]-silodosin* pK_i	*[^{3}H]-prazosin* $pK_{i\,high}$ *(%high)*	$pK_{i\,low}$
Prazosin	9.8 ± 0.2	9.9 ± 0.1	
Silodosin	9.9 ± 0.1	10.0 ± 0.2 (55 ± 5%)	7.5 ± 0.2
Tamsulosin	10.0 ± 0.1	9.8 ± 0.2	
BMY 7378	6.3 ± 0.2	6.4 ± 0.1	
RS-17053	8.7 ± 0.3	8.8 ± 0.3 (59 ± 4%)	7.8 ± 0.3
5-Methylurapidil	9.0 ± 0.2	8.9 ± 0.3 (60 ± 4%)	7.4 ± 0.2

Abbreviations: %high, proportion of high affinity sites; $pK_{i\,high}$ and $pK_{i\,low}$, negative logarithm of the equilibrium constants (pK_i) at high and low affinity sites for tested drugs.
Intact tissue segment binding experiments were carried out at 200 pM [^{3}H]-silodosin or 500 pM [^{3}H]-prazosin. Data represent mean ± s.e.mean of 4–5 experiments.

α_{1A}- and α_{1B}-ARs showing a high affinity for prazosin has previously been found in conventional membrane binding assays with [^{3}H]-prazosin (Morrow and Creese, 1986; Hanft and Gross, 1989; Yang *et al*., 1997). These findings were confirmed in the [^{3}H]-prazosin binding experiments using rat cerebral cortex membranes in the present study. However, we recently noticed that some native profiles of receptors could not be detected after the homogenization, as homogenization for membrane preparation may perturb the receptor environment (Muramatsu *et al*., 2005). Therefore, in the hope that the other subtypes of α_1-ARs could be identified in addition to α_{1A} and α_{1B} subtypes, we conducted radioligand binding assays with intact tissue segments of rat cerebral cortex.

Both [^{3}H]-silodosin and [^{3}H]-prazosin bound to the intact segments of rat cerebral cortex in a single population. However, the B_{max} and pharmacological profiles of the binding sites were apparently different between both radioligands, suggesting that the detection of different populations of α_1-ARs is dependent on the radioligand used (Figure 3a). The [^{3}H]-silodosin binding sites in intact tissue segments were divided into two distinct components having different affinities for prazosin, RS-17053 and 5-methylurapidil but not for silodosin, tamsulosin and BMY 7378, whereas the [^{3}H]-prazosin binding sites showed different affinities for silodosin, RS-17053 and 5-methylurapidil but not for prazosin (Table 1). Selectivity of these drugs for α_1-AR subtypes is now interpreted as follows: silodosin selective for α_{1A} and α_{1L} subtypes (Murata *et al*., 1999, 2000; Hiraizumi-Hiraoka *et al*., 2004), tamsulosin selective for all α_1-AR subtypes or with slightly low affinity for the α_{1B} subtype (Testa *et al*., 1997; Muramatsu *et al*., 1998b), prazosin selective for α_{1A}, α_{1B} and α_{1D} subtypes (Hancock, 1996; Murata *et al*., 1999; Hiraizumi-Hiraoka *et al*., 2004), RS-17053 and 5-methylurapidil selective for α_{1A} subtypes (Hanft and Gross, 1989; Ford *et al*., 1996; Rokosh and Simpson, 2002), and BMY 7378 selective for the α_{1D} subtype (Goetz *et al*., 1995). According to these criteria for α_1-AR subclassification, it is likely that [^{3}H]-silodosin binding sites in the intact tissue segments of rat cerebral cortex are composed of α_{1A} and α_{1L}-AR subtypes, whereas the [^{3}H]-prazosin binding sites are characterized as α_{1A} and α_{1B} subtypes (Figure 3a).

The failure to detect the α_{1L}-AR at [^{3}H]-prazosin binding sites in the cerebral cortex segments may be due to the subnanomolar concentrations of [^{3}H]-prazosin used in the present study, as the affinity of prazosin to α_{1L}-AR is approximately 100 times lower than that to the other α_1-AR subtypes (Table 1). Higher concentrations of [^{3}H]-prazosin could not be used in the tissue segment binding assay, as the proportion of nonspecific binding sites would become too high (Figure 4a). The inability to detect α_{1B}-ARs with [^{3}H]-silodosin also seemed to be due to its low affinity for α_{1B}-ARs.

The same number of α_{1A}-ARs was estimated when either [^{3}H]-silodosin or [^{3}H]-prazosin was used to determine binding sites in the intact segments of cerebral cortex (Figure 3a). This suggests that α_{1A}-ARs (and probably other α_1-AR subtypes) occurring in the intact tissue segments can be detected as independent entities and without loss, even though different radioligands are used (Figure 3a). However, α_{1D}-AR, which shows a high affinity for BMY 7378, was not detected, even though the expression of its corresponding mRNA has been demonstrated in this tissue (Pieribone *et al*., 1994; Day *et al*., 1997). The inability to detect α_{1D}-ARs is consistent with results from a previous study performed with the conventional membrane binding method (Yang *et al*., 1997).

One of the most interesting findings in the present study is that α_{1L}-AR could be clearly detected only at the [^{3}H]-silodosin binding sites of the intact segments but not in the membrane preparations of rat cortex. That is, the binding profile of the α_{1L}-AR disappeared in the membrane preparations and only an α_{1A}-AR-like profile was apparent in these preparations. As the number of [^{3}H]-silodosin binding sites (estimated as the amount per total tissue protein; Figure 3a) was not significantly different between the intact segments and the membrane preparations, it is assumed that the lack of α_{1L}-AR in the membranes represents a change in the binding profile of α_{1L}-AR to α_{1A}-AR upon/after homogenization. In order to confirm this possibility, the binding sites of [^{3}H]-prazosin in the intact tissue segments and in the membranes were also examined and compared. If α_{1L}-AR does convert to the α_{1A}-AR or, strictly speaking, into a receptor with a profile similar to the α_{1A}-AR, the converted component would be detected as additional binding sites of [^{3}H]-prazosin, resulting in an increase in the B_{max} in the membranes. In contrast, if α_{1L}-AR still remains unchanged after homogenization and keeps its pharmacological profiles, [^{3}H]-prazosin at the concentrations used in conventional membrane binding studies would not be sufficient to be able to bind to the α_{1L} receptors in the membranes. The results obtained from the binding experiments with [^{3}H]-prazosin clearly showed a significant increase in the B_{max} value after homogenization and further revealed that the increase mostly consisted of an α_{1A}-AR-like component, as determined by a competition study with silodosin (Figure 3a). Competition binding experiments with RS-17053 and 5-methylurapidil using [^{3}H]-prazosin with membrane preparations also showed that the proportion of high-affinity sites for these antagonists was similar to that for silodosin, further suggesting that the significant increase in the B_{max} value after homogenization consists of α_{1A}-ARs. These results further support our hypothesis that the α_{1L}-ARs, which were detected in [^{3}H]-silodosin tissue segment bindings as the low-affinity sites for prazosin, show an α_{1A}(-like) profile in membrane preparations. Thus, a possible conversion of pharmacological profiles from α_{1L} subtype to α_{1A} subtype may be suggested from the present study. Alternatively, the increase in [^{3}H]-prazosin binding sites or α_{1A}-ARs in the membrane preparations may be related to an additional detection of intracellular receptors, because α_1-ARs have been shown to be present not only at the surface but also intracellularly (MacKenzie *et al*., 2000). If the latter case occurs, approximately 40% of α_{1A}-ARs should distribute intracellularly under intact tissue conditions, and also the plasma membrane α_{1L}-ARs should be easily decomposed by homogenization.

In contrast to the cerebral cortex, [^{3}H]-silodosin binding to the segments of rat tail artery was monophasically antagonized by all the competitors tested, and the pharmacological profile corresponded to that of α_{1A}-ARs. The lack of α_{1L}-ARs in the tail artery is consistent with results obtained in functional bioassays, where α_{1A}-AR was predominantly involved in adrenergic contractions (Lachnit *et al*., 1997). The present results in the tail artery further imply that α_{1L}-AR is not necessarily expressed concomitant with α_{1A}-AR, as suggested in previous functional studies (Muramatsu *et al*., 1995).

Compared to the [^{3}H]-silodosin binding sites, the [^{3}H]-prazosin binding sites in the segments of rat tail artery were higher in density and were composed of two components (α_{1A}- and α_{1B}-ARs), which were differentiated by silodosin, RS-17053 or 5-methylurapidil, as demonstrated previously (Tanaka *et al*., 2004). Furthermore, the number of α_{1A}-ARs calculated at [^{3}H]-prazosin binding sites was in good agreement with the density of [^{3}H]-silodosin binding sites (Figure 3b). Thus, the results in the tail artery also reveal that the intact tissue segment binding assay can recognize various α_1-ARs as distinct entities.

Many research groups have tried to clone α_{1L}-AR, but its gene has not yet been found. Rather, Ford *et al*. (1997) proposed that α_{1L}-AR is a possible phenotype of α_{1A}-AR, as they demonstrated that the α_{1A}-ARs expressed in Chinese hamster ovary cells have an α_{1L} profile in functional and binding studies, although these findings were not confirmed by other groups (Taniguchi *et al*., 1999; Stanasila *et al*., 2003; Israilova *et al*., 2004; Ramsay *et al*., 2004). Our tissue segment binding studies have demonstrated that α_{1L}-AR coexists with α_{1A}-AR as a pharmacologically distinct entity (present study, Hiraizumi-Hiraoka *et al*., 2004; Morishima *et al*., 2007). Therefore, it might be supposed that the α_{1A}-*AR* gene products can express both α_{1A}- and α_{1L}-AR phenotypes in several organs when the tissues are kept intact and that one isoform (α_{1L}-AR) can be more dramatically affected by homogenization, resulting in either its disappearance or a change of its profile to the other (α_{1A}-AR). Disturbance of the natural receptor environment upon tissue homogenization might be one of the reasons that the binding in membrane preparations would not necessarily reflect the binding to native types of receptor present in intact tissues (Bylund and Toews, 1993; Hiraizumi-Hiraoka *et al*., 2004; Tanaka *et al*., 2004). With this in mind, it may be interesting to note that

distinct antagonist affinities have been found between membrane binding and functional bioassay (Van der Graaf *et al*., 1996; Stam *et al*., 1999; Nelson and Challiss, 2007).

With regard to the hypothesis mentioned above, it is interesting to refer to the two distinct states of β_1-ARs (β1H and β_{1L} ARs), which show different sensitivities to some drugs in spite of having the same gene products (Sarsero *et al*., 2003; Molenaar and Parsonage, 2005). More recently, evidence has been obtained showing that the same receptor gene products may express different phenotypes that exhibit different antagonist pharmacology in different tissues (Nelson and Challiss, 2007). The underlying mechanisms that determine the expression of two distinct α_1-AR phenotypes have now been examined by our group.

In conclusion, the present binding study with rat cerebral cortex showed that α_{1L}-AR can be detected as a pharmacologically distinct entity from α_{1A}-, α_{1B}- and α_{1D}-ARs in intact tissues and that α_{1L}-ARs disappear after tissue homogenization. This may be one of the reasons why α_{1L}-ARs are difficult to detect in membrane preparations subjected to conventional binding techniques but can be demonstrated in functional bioassays that use intact tissue segments.

Acknowledgements

This work was supported in part by a Grant-in-Aid for Scientific Research and the 21st COE Research Program (Medical Science) from the Ministry of Education, Culture, Sports, Science and Technology of Japan and by a grant from the Smoking Research Foundation of Japan.

Conflict of interest

The authors state no conflict of interest.

References

Amobi NI, Guillebaud J, Kaisary AV, Turner E, Smith IC (2002). Discrimination by SZL49 between contractions evoked by noradrenaline in longitudinal and circular muscle of human vas deferens. *Br J Pharmacol* **136**: 127–135.

Argyle SA, McGrath JC (2000). An alpha(1A)/alpha(1L)-adrenoceptor mediates contraction of canine subcutaneous resistance arteries. *J Pharmacol Exp Ther* **295**: 627–633.

Bylund DB, Toews ML (1993). Radioligand binding methods: practical guide and tips. *Am J Physiol* **265**: L421–L429.

Day HE, Campeau S, Watson Jr SJ, Akil H (1997). Distribution of alpha 1a-, alpha 1b- and alpha 1d-adrenergic receptor mRNA in the rat brain and spinal cord. *J Chem Neuroanat* **13**: 115–139.

Ford AP, Arredondo NF, Blue Jr DR, Bonhaus DW, Jasper J, Kava MS *et al*. (1996). RS-17053 (*N*-[2-(2-cyclopropylmethoxyphenoxy) ethyl]-5-chloro-alpha, alpha-dimethyl-1*H*-indole-3-ethanamine hydrochloride), a selective alpha 1A-adrenoceptor antagonist, displays low affinity for functional alpha 1-adrenoceptors in human prostate: implications for adrenoceptor classification. *Mol Pharmacol* **49**: 209–215.

Ford AP, Daniels DV, Chang DJ, Gever JR, Jasper JR, Lesnick JD *et al*. (1997). Pharmacological pleiotropism of the human recombinant alpha1A-adrenoceptor: implications for alpha1-adrenoceptor classification. *Br J Pharmacol* **121**: 1127–1135.

Goetz AS, King HK, Ward SD, True TA, Rimele TJ, Saussy Jr DL (1995). BMY 7378 is a selective antagonist of the D subtype of alpha 1-adrenoceptors. *Eur J Pharmacol* **272**: R5–R6.

Hancock AA (1996). Alpha1 Adrenoceptor subtypes: a synopsis of their pharmacology and molecular biology. *Drug Dev Res* **39**: 54–107.

Hanft G, Gross G (1989). Subclassification of alpha 1-adrenoceptor recognition sites by urapidil derivatives and other selective antagonists. *Br J Pharmacol* **97**: 691–700.

Hieble JP, Bylund DB, Clarke DE, Eikenburg DC, Langer SZ, Lefkowitz RJ *et al*. (1995). International Union of Pharmacology. X. Recommendation for nomenclature of alpha 1-adrenoceptors consensus update. *Pharmacol Rev* **47**: 267–270.

Hieble JP (2000). Adrenoceptor subclassification: an approach to improved cardiovascular therapeutics. *Pharm Acta Helv* **74**: 163–171.

Hiraizumi-Hiraoka Y, Tanaka T, Yamamoto H, Suzuki F, Muramatsu I (2004). Identification of alpha-1L adrenoceptor in rabbit ear artery. *J Pharmacol Exp Ther* **310**: 995–1002.

Hiraoka Y, Ohmura T, Oshita M, Watanabe Y, Morikawa K, Nagata O *et al*. (1999). Binding and functional characterization of alpha1-adrenoceptor subtypes in the rat prostate. *Eur J Pharmacol* **366**: 119–126.

Hiraoka Y, Ohmura T, Sakamoto S, Hayashi H, Muramatsu I (1995). Identification of alpha 1-adrenoceptor subtypes in the rabbit prostate. *J Auton Pharmacol* **15**: 271–278.

Honner V, Docherty JR (1999). Investigation of the subtypes of alpha1-adrenoceptor mediating contractions of rat vas deferens. *Br J Pharmacol* **128**: 1323–1331.

Israilova M, Tanaka T, Suzuki F, Morishima S, Muramatsu I (2004). Pharmacological characterization and cross talk of alpha1a- and alpha1b-adrenoceptors coexpressed in human embryonic kidney 293 cells. *J Pharmacol Exp Ther* **309**: 259–266.

Kenny B, Ballard S, Blagg J, Fox D (1997). Pharmacological options in the treatment of benign prostatic hyperplasia. *J Med Chem* **40**: 1293–1315.

Lachnit WG, Tran AM, Clarke DE, Ford AP (1997). Pharmacological characterization of an alpha 1A-adrenoceptor mediating contractile responses to noradrenaline in isolated caudal artery of rat. *Br J Pharmacol* **120**: 819–826.

Mackenzie JF, Daly CJ, Pediani JD, McGrath JC (2000). Quantitative imaging in live human cells reveals intracellular alpha(1)-adrenoceptor ligand-binding sites. *J Pharmacol Exp Ther* **294**: 434–443.

Michel MC, Kenny B, Schwinn DA (1995). Classification of alpha 1-adrenoceptor subtypes. *Naunyn Schmiedebergs Arch Pharmacol* **352**: 1–10.

Michelotti GA, Price DT, Schwinn DA (2000). Alpha 1-adrenergic receptor regulation: basic science and clinical implications. *Pharmacol Ther* **88**: 281–309.

Molenaar P, Parsonage WA (2005). Fundamental considerations of beta-adrenoceptor subtypes in human heart failure. *Trends Pharmacol Sci* **26**: 368–375.

Morishima S, Tanaka T, Yamamoto H, Suzuki F, Akino H, Yokoyama O *et al*. (2007). Identification of alpha-1L and alpha-1A adrenoceptors in human prostate by tissue segment binding. *J Urol* **177**: 377–381.

Morrow AL, Creese I (1986). Characterization of alpha 1-adrenergic receptor subtypes in rat brain: a reevaluation of [^{3}H]WB4104 and [^{3}H]prazosin binding. *Mol Pharmacol* **29**: 321–330.

Muramatsu I, Murata S, Isaka M, Piao HL, Zhu J, Suzuki F *et al*. (1998a). Alpha1-adrenoceptor subtypes and two receptor systems in vascular tissues. *Life Sci* **62**: 1461–1465.

Muramatsu I, Ohmura T, Kigoshi S, Hashimoto S, Oshita M (1990). Pharmacological subclassification of alpha 1-adrenoceptors in vascular smooth muscle. *Br J Pharmacol* **99**: 197–201.

Muramatsu I, Ohmura T, Hashimoto S, Oshita M (1995). Functional subclassification of vascular alpha1 adrenoceptors. *Pharmacol Commun* **6**: 23–28.

Muramatsu I, Oshita M, Ohmura T, Kigoshi S, Akino H, Gobara M *et al*. (1994). Pharmacological characterization of alpha 1-adrenoceptor subtypes in the human prostate: functional and binding studies. *Br J Urol* **74**: 572–578.

Muramatsu I, Tanaka T, Suzuki F, Li Z, Hiraizumi-Hiraoka Y, Anisuzzaman AS *et al*. (2005). Quantifying receptor properties:

the tissue segment binding method—a powerful tool for the pharmacome analysis of native receptors. *J Pharmacol Sci* **98**: 331–339.

Muramatsu I, Taniguchi T, Okada K (1998b). Tamsulosin: alpha1-adrenoceptor subtype-selectivity and comparison with terazosin. *Jpn J Pharmacol* **78**: 331–335.

Murata S, Taniguchi T, Muramatsu I (1999). Pharmacological analysis of the novel, selective alpha1-adrenoceptor antagonist, KMD-3213, and its suitability as a tritiated radioligand. *Br J Pharmacol* **127**: 19–26.

Murata S, Taniguchi T, Takahashi M, Okada K, Akiyama K, Muramatsu I (2000). Tissue selectivity of KMD-3213, an alpha(1)-adrenoreceptor antagonist, in human prostate and vasculature. *J Urol* **164**: 578–583.

Nakamura S, Taniguchi T, Suzuki F, Akagi Y, Muramatsu I (1999). Evaluation of α_1-adrenoceptors in the rabbit iris: pharmacological characterization and expression of mRNA. *Br J Pharmacol* **127**: 1367–1374.

Nelson CP, Challiss RA (2007). 'Phenotypic' pharmacology: the influence of cellular environment on G protein-coupled receptor antagonist and inverse agonist pharmacology. *Biochem Pharmacol* **73**: 737–751.

Ohmura T, Oshita M, Kigoshi S, Muramatsu I (1992). Identification of alpha 1-adrenoceptor subtypes in the rat vas deferens: binding and functional studies. *Br J Pharmacol* **107**: 697–704.

Oshita M, Kigoshi S, Muramatsu I (1993). Pharmacological characterization of two distinct alpha 1-adrenoceptor subtypes in rabbit thoracic aorta. *Br J Pharmacol* **108**: 1071–1076.

Pieribone VA, Nicholas AP, Dagerlind A, Hokfelt T (1994). Distribution of alpha 1 adrenoceptors in rat brain revealed by *in situ* hybridization experiments utilizing subtype-specific probes. Distribution of alpha 1 adrenoceptors in rat brain revealed by *in situ* hybridization experiments utilizing subtype-specific probes. *J Neurosci* **14**: 4252–4268.

Ramsay D, Carr IC, Pediani J, Lopez-Gimenez JF, Thurlow R, Fidock M *et al*. (2004). High-affinity interactions between human alpha1A-adrenoceptor C-terminal splice variants produce homo- and heterodimers but do not generate the alpha1L-adrenoceptor. *Mol Pharmacol* **66**: 228–239.

Rokosh DG, Simpson PC (2002). Knockout of the alpha 1A/C-adrenergic receptor subtype: the alpha 1A/C is expressed in resistance arteries and is required to maintain arterial blood pressure. *Proc Natl Acad Sci USA* **99**: 9474–9479.

Sarsero D, Russell FD, Lynham JA, Rabnott G, Yang I, Fong KM *et al*. (2003). (-)-CGP 12177 increases contractile force and hastens relaxation of human myocardial preparations through a propranolol-resistant state of the beta 1-adrenoceptor. *Naunyn Schmiedebergs Arch Pharmacol* **367**: 10–21.

Stam WB, Van der Graaf PH, Saxena PR (1999). Analysis of alpha 1L-adrenoceptor pharmacology in rat small mesenteric artery. *Br J Pharmacol* **127**: 661–670.

Stanasila L, Perez JB, Vogel H, Cotecchia S (2003). Oligomerization of the alpha 1a- and alpha 1b-adrenergic receptor subtypes. Potential implications in receptor internalization. *J Biol Chem* **278**: 40239–40251.

Suzuki F, Taniguchi T, Nakamura S, Akagi Y, Kubota C, Satoh M *et al*. (2002). Distribution of alpha-1 adrenoceptor subtypes in RNA and protein in rabbit eyes. *Br J Pharmacol* **135**: 600–608.

Taki N, Tanaka T, Zhang L, Suzuki F, Israilova M, Taniguchi T *et al*. (2004). Alpha-1D adrenoceptors are involved in reserpine-induced supersensitivity of rat tail artery. *Br J Pharmacol* **142**: 647–656.

Tanaka T, Zhang L, Suzuki F, Muramatsu I (2004). Alpha-1 adrenoceptors: evaluation of receptor subtype-binding kinetics in intact arterial tissues and comparison with membrane binding. *Br J Pharmacol* **141**: 468–476.

Taniguchi T, Inagaki R, Murata S, Akiba I, Muramatsu I (1999). Microphysiometric analysis of human alpha1a-adrenoceptor expressed in Chinese hamster ovary cells. *Br J Pharmacol* **127**: 962–968.

Testa R, Guarneri L, Angelico P, Poggesi E, Taddei C, Sironi G *et al*. (1997). Pharmacological characterization of the uroselective alpha-1 antagonist Rec 15/2739 (SB 216469): role of the alpha-1L adrenoceptor in tissue selectivity, part II. *J Pharmacol Exp Ther* **281**: 1284–1293.

Van der Graaf PH, Shankley NP, Black JW (1996). Analysis of the activity of alpha 1-adrenoceptor antagonists in rat aorta. *Br J Pharmacol* **118**: 299–310.

Van der Graaf PH, Deplanne V, Duquenne C, Angel I (1997). Analysis of alpha1-adrenoceptors in rabbit lower urinary tract and mesenteric artery. *Eur J Pharmacol* **327**: 25–32.

Yang M, Verfurth F, Buscher R, Michel MC (1997). Is alpha1D-adrenoceptor protein detectable in rat tissues? *Naunyn Schmiedebergs Arch Pharmacol* **355**: 438–446.

Zhong H, Minneman KP (1999). Alpha1-adrenoceptor subtypes. *Eur J Pharmacol* **375**: 261–276.